

Structure-Function Analysis of Vitamin D 24-Hydroxylase (CYP24A1) by Site-Directed Mutagenesis: Amino Acid Residues Responsible for Species-Based Difference of CYP24A1 between Humans and Rats

Hiromi Hamamoto, Tatsuya Kusudo, Naoko Urushino, Hiroyuki Masuno, Keiko Yamamoto, Sachiko Yamada, Masaki Kamakura, Miho Ohta, Kuniyo Inouye, and Toshiyuki Sakaki

Division of Food Science and Biotechnology, Graduate School of Agriculture, Kyoto University, Kyoto, Japan (H.H., T.K., N.U., K.I.); Institute of Biomaterials and Bioengineering, Tokyo Medical and Dental University, Tokyo, Japan (H.M., K.Y., S.Y.); Biotechnology Research Center, Faculty of Engineering, Toyama Prefectural University, Toyama, Japan (M.K., T.S.); and Laboratory of Nutrition, Koshien University, Nishinomiya, Japan (M.O.)

Received February 7, 2006; accepted April 13, 2006

ABSTRACT

Our previous studies revealed the species-based difference of CYP24A1-dependent vitamin D metabolism. Although human CYP24A1 catalyzes both C-23 and C-24 oxidation pathways, rat CYP24A1 shows almost no C-23 oxidation pathway. We tried to identify amino acid residues that cause the species-based difference by site-directed mutagenesis. In the putative substrate-binding regions, amino acid residue of rat CYP24A1 was converted to the corresponding residue of human CYP24A1. Among eight mutants examined, T416M and I500T showed C-23 oxidation pathway. In addition, the mutant I500F

showed quite a different metabolism of $1\alpha,25$ -dihydroxyvitamin D_3 [$1\alpha,25(OH)_2D_3$] from both human and rat CYP24A1. These results strongly suggest that the amino acid residues at positions 416 and 500 play a crucial role in substrate binding and greatly affect substrate orientation. A three-dimensional model of CYP24A1 indicated that the A-ring and triene part of $1\alpha,25(OH)_2D_3$ could be located close to amino acid residues at positions 416 and 500, respectively. Our findings provide useful information for the development of new vitamin D analogs for clinical use.

The hormonally active form of vitamin D_3 , $1\alpha,25(OH)_2D_3$, plays essential roles in calcium homeostasis, immune response, and cell differentiation (Boyle et al., 1971; Holick et al., 1971; Lawson et al., 1971; Norman et al., 1971; Bouillon et al., 1995). A large number of vitamin D analogs have been synthesized for clinical use in type I rickets, osteoporosis, renal osteodystrophy, psoriasis, leukemia, and breast cancer, and their biological activity has been evaluated. Much research has investigated the biological mechanism of vitamin D analogs, revealing that the biological activities of analogs are due not only to the analog itself but also to its metabolites (Binderup et al., 1991; Binderup, 1992; Dilorth et al., 1997). CYP24A1 plays a central role in the metabolism of $1\alpha,25(OH)_2D_3$ and its analogs in target tissues such as kid-

neys, intestines, and bones. A species-based difference has been revealed in the CYP24A1-dependent metabolism of $1\alpha,25(OH)_2D_3$ between rats and humans (Akiyoshi-Shibata et al., 1994; Beckman et al., 1996; Sakaki et al., 1999, 2000). Human CYP24A1 demonstrated a remarkable metabolism consisting of both C-23 and C-24 oxidation pathways, whereas rat CYP24A1 showed extreme predominance of C-24 over C-23 oxidation pathways. In addition, a remarkable species-based difference was also observed in the CYP24A1-dependent metabolism of vitamin D analogs (Sakaki et al., 2003; Kusudo et al., 2003, 2004; Abe et al., 2005). These facts suggest that preclinical tests using such animals as rats and mice cannot correctly predict the metabolism of vitamin D analogs in the human body. Thus, information on substrate recognition, the reaction mechanism, and the species-based difference of CYP24A1 seems quite useful to develop vitamin D analogs for clinical use. Another area of CYP24A1 research with pharmacological interest is development of specific inhibitor of CYP24A1 (Schuster et al., 2003; Kahraman et al.,

This work was supported in part by a Grant-in-Aid for Scientific Research from the Ministry of Education, Science and Culture of Japan, and Sankyo Foundation of Life Sciences.

Article, publication date, and citation information can be found at <http://molpharm.aspetjournals.org>.
doi:10.1124/mol.106.023275.

ABBREVIATIONS: $1\alpha,25(OH)_2D_3$, $1\alpha,25$ -dihydroxyvitamin D_3 ; ADR, NADPH-adrenodoxin reductase; HPLC, high-performance liquid chromatography; SRS, substrate recognition sites.

2004). Blockers of CYP24A1 might extend the half-life of $1\alpha,25(\text{OH})_2\text{D}_3$ and its analogs within target cells, especially cells that overexpress CYP24A1. In addition, in this case, information on tertiary structure of substrate-binding pocket of CYP24A1 is quite useful to develop specific inhibitors of CYP24A1. The tertiary structure of CYP24A1 has been proposed by molecular modeling (Omdahl et al., 2003).

So far, crystal structures of more than ten prokaryotic P450s and four mammalian microsomal P450s have been solved (Williams et al., 2000, 2003, 2004; Scott et al., 2003; Wester et al., 2003; Schoch et al., 2004; Yano et al., 2005; Rowland et al., 2006). The overall folding of those P450s is quite similar, although their sequence identity is less than 20%. These findings strongly suggest that mitochondrial P450s have structural folding similar to that of prokaryotic soluble and microsomal P450s. We have constructed tertiary structure of CYP27B1 by a homology modeling technique using the structure of CYP2C5 as a template (Yamamoto et al., 2004, 2005). The resultant three-dimensional model of CYP27B1 provided an opportunity to understand the spatial location and function of the residues responsible for mutations with vitamin D-dependent rickets type I. Using the three-dimensional model, we studied the docking of 25-hydroxyvitamin D_3 into the substrate-binding pocket of CYP27B1 and predicted that Thr409 of human CYP27B1 is responsible for substrate binding. Thus, a homology modeling technique together with mutation study gives useful information on the structure-function analysis of mitochondrial P450s.

In this study, we attempted to construct three-dimensional model of CYP24A1 to understand structure-function relationship of CYP24A1. The enzymatic properties of CYP24A1 mutants constructed by site-directed mutagenesis were examined to determine the amino acid residues responsible for the species-based difference of CYP24A1 between humans and rats.

Materials and Methods

Materials. DNA-modifying enzymes and restriction enzymes were purchased from Takara Shuzo Co., Ltd. (Kyoto, Japan). $1\alpha,25(\text{OH})_2\text{D}_3$ was purchased from Wako Pure Chemical Industries, Ltd. (Osaka, Japan). NADPH was purchased from Oriental Yeast Co. (Tokyo, Japan). Bovine NADPH-adrenodoxin reductase (ADR) and adrenodoxin were kind gifts from Dr. Y. Nonaka (Koshien University, Nishinomiya, Japan). Terrific broth was purchased from Invitrogen (Paisley, UK). *Escherichia coli* JM109 (Takara Shuzo, Kyoto, Japan) was used as a host strain. Other chemicals used were of the highest quality commercially available.

Sequence Alignment and Homology Modeling. Rat CYP24A1, human CYP24A1, and rabbit microsomal CYP2C5 were aligned by using ClustalW interfaced with ClustalX for Windows (ver 1.81). According to the alignment, we constructed three-dimensional models of human CYP24A1 and rat CYP24A1 by using SYBYL modeling software, COMPOSER (Tripos Inc., St. Louis, MO), and the atomic coordinate of the crystal structure of rabbit CYP2C5 as a template (Williams et al., 2000; Wester et al., 2003). Modeling procedures are summarized below.

1. The structure of the structurally conserved regions (SCR) (all helices, β -sheets, and loops having the same number of amino acid residues) was constructed.
2. Backbone structure of the residual parts was constructed with the loop search command of SYBYL and the selected loops were joined to the SCR parts; their side chains were then added.

3. Heme was merged into the protein as it adopts the same spatial location as the heme of the template CYP2C5.
4. Hydrogens were added to the model structure.
5. The constructed structure was optimized in added water by the precomputed box method (Tripos force field). Optimization was carried out in the following order of consideration: loop regions, side chains, and the whole molecule. Each energy minimization was carried out 5000 iterations. The model structure was evaluated by PROCHECK Program.
6. $1\alpha,25(\text{OH})_2\text{D}_3$ was manually docked into CYP24A1 model based on the experimental results of site-directed mutagenesis described below.

Substrate Docking. The substrate, $1\alpha,25(\text{OH})_2\text{D}_3$, was manually docked into CYP24A1 model based on experimental results of the site-directed mutagenesis.

1. $1\alpha,25(\text{OH})_2\text{D}_3$ was put into the substrate binding pocket, as the triene part was located near the important residues, Ile500 and Thr416, for regioselectivity of the side-chain hydroxylation and C(23)- and C(24)-positions of the side chain were near the Fe of the heme.
2. Optimization of the resultant docking model was performed on the Tripos force field, in which the protein part was fixed.
3. We selected one $1\alpha,25(\text{OH})_2\text{D}_3$ -CYP24A1 complex model in which $1\alpha,25(\text{OH})_2\text{D}_3$ adopted its stable conformation.

Site-Directed Mutagenesis. The mutated amino acid residues and their putative locations are summarized in Table 1. Mutants were generated by QuikChange site-directed mutagenesis kit (Stratagene, La Jolla, CA) according to the instruction manual. The oligonucleotide primers for mutagenesis are shown in Table 2. Corrected generation of desired mutations was confirmed by DNA sequencing.

TABLE 1
Oligonucleotides used to generate CYP24A1 mutants
The mutated nucleotides are underlined.

| Mutation | Oligonucleotides |
|----------|---|
| H125Y | 5'-ACAGAGAGCGCGTATCCCCAGCGACTG-3' 5'-CAGTCGCTGGGGATACGCGCTCTCTGT-3' |
| H140Y | 5'-GGAAAGCCTATCGCGACTACAGGAACGAAG-3' 5'-CTTCGTTCCCTGTAGTCGCGATAGGCTTTCC-3' |
| N142K | 5'-CTATCGCGACCACAGGAAAGAGCCTACG-3' 5'-CGTAGGCTTCTTTCTGTGGTCGCGATAG-3' |
| R262S | 5'-GTTGCACAAGAGCCTCAACACCAAAG-3' 5'-CTTTGGTGTGAGGCTCTTGTGCAAC-3' |
| A270D | 5'-CAAAGTGTGGCAGGACCATACGCTG-3' 5'-CAGGCGTATGCTCCTGCCACACTTTG-3' |
| T416M | 5'-GGAACAGTGTAAATGCTCAATACCCA-3' 5'-TGGGTATTGAGCATTAACACTGTTCC-3' |
| T416A | 5'-GGAACAGTGTAAATGCTCAATACCCA-3' 5'-TGGGTATTGAGGCTTAACACTGTTCC-3' |
| T416S | 5'-GGAACAGTGTAAATGCTCAATACCCA-3' 5'-TGGGTATTGAGGCTTAACACTGTTCC-3' |
| T416V | 5'-GGAACAGTGTAAATGCTCAATACCCA-3' 5'-TGGGTATTGAGGCTTAACACTGTTCC-3' |
| T416I | 5'-GGAACAGTGTAAATGCTCAATACCCA-3' 5'-TGGGTATTGAGGCTTAACACTGTTCC-3' |
| T416F | 5'-GGAACAGTGTAAATGCTCAATACCCA-3' 5'-TGGGTATTGAGGCTTAACACTGTTCC-3' |
| L498S | 5'-GATGCTGCACCTTGGCATCTG-3' 5'-CAGGATGCCAGAGTCGAGCATC-3' |
| I500T | 5'-CTTGGCACTCCTGGTACCC-3' 5'-TACCAGGTCGCAAGGTG-3' |
| I500A | 5'-CTTGGCCCTCCTGGTACCC-3' 5'-TACCAGGTCGCAAGGTG-3' |
| I500V | 5'-CTTGGCTCCTGGTACCC-3' 5'-TACCAGGTCGCAAGGTG-3' |
| I500L | 5'-CTTGGCTCCTGGTACCC-3' 5'-TACCAGGTCGCAAGGTG-3' |
| I500F | 5'-CTTGGCTCCTGGTACCC-3' 5'-TACCAGGTCGCAAGGTG-3' |

Cultivation of the Recombinant *E. coli* Cells. Recombinant *E. coli* cells were grown in TB broth containing 50 $\mu\text{g/ml}$ ampicillin at 26°C under good aeration. The induction of transcription of CYP24A1 cDNA under tac promoter was initiated by the addition of isopropyl-thio- β -D-galactopyranoside at final concentration of 1 mM when the cell density (A_{660}) reached 0.5. δ -Aminolevulinic acid was also added at a final concentration of 0.5 mM. The recombinant cells were gently shaken at 26°C under good aeration by bubbling as described previously (Akiyoshi-Shibata et al., 1994).

Preparation of Membrane Fraction. Subcellular fractionation of *E. coli* cells was carried out basically according to our previous study (Akiyoshi-Shibata et al., 1994). Tris-HCl buffer (100 mM, pH 7.4) was used for suspension of the membrane fraction.

Measurement of Reduced CO Difference Spectra. The reduced CO-difference spectra were measured with a Shimadzu UV-2200 spectrophotometer (Kyoto, Japan) (Omura and Sato, 1994; Kondo et al., 1999). The absorption-coefficient difference between 445 nm and 490 nm ($\Delta\epsilon_{445-490}$) = 105 $\text{mM}^{-1} \text{cm}^{-1}$ was used for the calculation of the P450 hemoprotein concentration, as described previously (Akiyoshi-Shibata et al., 1994).

Measurement of Enzyme Activity of CYP24A1. The activity toward $1\alpha,25(\text{OH})_2\text{D}_3$ was measured in the reconstituted system containing the membrane fraction 10 to 30 nM CYP24A1, 2 μM adrenodoxin, 0.2 μM NADPH-adrenodoxin reductase (ADR), 4 μM substrate, 100 mM Tris-HCl, pH 7.4, and 1 mM EDTA in a final volume of 0.5 ml. For the determination of apparent kinetic parameters, the reaction mixture consisting of the membrane fraction containing 10 to 30 nM CYP24A1 or its mutant, 0.1 μM adrenodoxin, 0.01 μM ADR, and 0 to 2.0 μM $1\alpha,25(\text{OH})_2\text{D}_3$. To determine K_m values correctly, the successive reaction by CYP24A1 should be avoided as described previously (Sakaki et al., 2000; Kusudo et al., 2004). Thus, the concentrations of adrenodoxin and ADR were extremely reduced. Under these conditions, the sum of 23(S)-hydroxylated and 24(R)-hydroxylated products of the substrate is more than 90% of total metabolites. The reaction was initiated by adding NADPH to a final concentration of 1 mM. Aliquots of the reaction mixture were collected after varying time intervals and extracted with four volumes of chloroform/methanol (3:1). The organic phase was recovered and dried up. The resulting residue was solubilized with acetonitrile and applied to HPLC under the following conditions: column, YMC-Pack ODS-AM (4.6 \times 300 mm) (YMC Co., Tokyo, Japan). UV detection, 265 nm; flow rate, 1.0 ml/min; column temperature, 40°C; mobile phase, a linear gradient from 20% to 100% acetonitrile in aqueous solution. The metabolites were also analyzed using a JASCO Finepak SIL-5 column (4.0 \times 25 mm; JASCO Co. Tokyo, Japan).

LC-MS Analysis of the Metabolites. Isolated metabolites from HPLC effluents were subjected to mass spectrometric analysis using a Finnegan Mat TSQ-70 with atmospheric pressure chemical ionization, positive mode. The conditions of LC were described below: column, reversed-phase ODS column (μ Bondapak C18, 5 μm ; Wa-

ters, Milford, MA) (6 \times 150 mm); mobile phase, 80% methanol aqueous solution per 25 min; flow rate, 1.0 ml/min; UV detection, 265 nm.

Other Methods. The concentration of vitamin D_3 derivatives was estimated by their molar extinction coefficient of $1.80 \times 10^4 \text{M}^{-1} \text{cm}^{-1}$ at 264 nm (Hiwatashi et al., 1982). Protein concentration was determined by the method of Lowry et al. (1951), using bovine serum albumin as a standard.

Results

Expression of the Mutants of Rat CYP24A1 in *E. coli* Cells. To determine the amino acid residues responsible for species-based difference of CYP24A1 between humans and rats, their amino acid sequences were compared. Figure 1 shows the alignment of amino acid sequences of human CYP24A1, rat CYP24A1, and CYP2C5, in which substrate recognition sites (SRS) proposed by Gotoh (1992) were indicated. The amino acid residues not conserved in both CYP24A1 in SRS regions were marked in Fig. 1. The seven amino acid residues of rat CYP24A1 were each mutated to the corresponding residues of human CYP24A1. Thus, the mutants H125Y, H140Y, N142K, R262S, A270D, L498S, and I500T were expressed in *E. coli* cells. In addition, mutants at 416 position were also constructed because Thr416 of rat CYP24A1 and Met 416 of human CYP24A1 seemed to be close to A-ring of $1\alpha,25(\text{OH})_2\text{D}_3$ based on the computer modeling. It should be noted that Thr416 corresponds to Thr409 of human CYP27B1, which is responsible for substrate-binding and whose mutation causes vitamin D-dependent rickets type I (Yamamoto et al., 2005). The expression level of human CYP24A1, rat CYP24A1, and its mutants except for T416M, T416V, and N142K was 50 to 100 nM culture, whereas the expression level of T416M, T416V, and N142K was 15 to 30 nmol/liter culture. All of the wild type and mutants CYP24A1 showed similar reduced CO-difference spectra with a maximum at around 445 nm.

Metabolism of $1\alpha,25(\text{OH})_2\text{D}_3$ by Human CYP24A1, Rat CYP24A1, and Its Mutants. The reconstituted system containing the membrane fraction prepared from the recombinant *E. coli* cells expressing wild-type or mutant CYP24A1, bovine adrenodoxin, and bovine ADR was examined for the metabolism of the $1\alpha,25(\text{OH})_2\text{D}_3$. Figure 2 shows metabolic pathways of $1\alpha,25(\text{OH})_2\text{D}_3$ catalyzed by CYP24A1 (Sawada et al., 2004). Figure 3 shows HPLC profiles of $1\alpha,25(\text{OH})_2\text{D}_3$ and their metabolites by human CYP24A1, rat CYP24A1, and its mutants. Based on our previous data on the metabolism of $1\alpha,25(\text{OH})_2\text{D}_3$, the metabolites were designated as follows $1\alpha,23\text{S},25,26(\text{OH})_4\text{D}_3$ (M1), 24-oxo-1,23,25(OH) $_3\text{D}_3$ (M2), 24,25,26,27-tetranor-1,23(OH) $_2\text{D}_3$ (M3), $1\alpha,23\text{S},25(\text{OH})_3\text{D}_3$ (M4), $1\alpha,24\text{R},25(\text{OH})_3\text{D}_3$ (M5), 24-oxo-1,25(OH) $_2\text{D}_3$ (M6), and 25,26,27-trinor-23-ene-1 $\alpha(\text{OH})\text{D}_3$ (M7) (Figs. 2 and 3). Note that the metabolites of C-23 oxidation pathway, M1 and M7, were detected in the metabolism by the mutants T416M and I500T (Figs. 3C and 4B). These results suggest that these mutants have the enzymatic properties similar to human CYP24A1. On the other hand, the mutants H125Y, H140Y, N142Y, R242S, A270D, and L498S showed nearly the same metabolism as rat CYP24A1. Table 2 shows the ratio between summed products of C-23 oxidation pathway (M1, M4, and M7) and those of C-24 oxidation pathway (M2, M3, M5, and M6) of metabolism by human CYP24A1, rat CYP24A1, and its mutants. The mutants H125Y, H140Y,

TABLE 2

The ratio of C-23 to C-24 oxidation pathways

The ratio between the summed products of C-23 pathway (M1, M4, M7) and those of C-24 pathway (M2, M3, M5, M6) is indicated.

| CYP24A1 | C-23/C-24 |
|---------|-----------|
| Rat | 0.01 |
| T416A | 0.01 |
| T416S | 0.01 |
| T416M | 0.08 |
| T416V | 0.16 |
| T416 I | 0.19 |
| T416F | 0.12 |
| I500A | 0.15 |
| I500V | 0.13 |
| I500T | 0.16 |
| I500L | 0.16 |
| Human | 0.27 |

N142K, R262S, A240D, and L498S showed the same C-23/-C-24 ratio, 0.01, as wild-type rat CYP24A1. However, it was demonstrated that single amino acid substitution at 416 or 500 dramatically increased the ratio of the C-23 to C-24 oxidation pathways (Table 2).

Molecular Modeling of CYP24A1. The overall folding of both rat CYP24A1 and human CYP24A1 was quite similar to those of CYP2C5 used as a template (Williams et al., 2000;

Wester et al., 2003) and three-dimensional model of CYP27B1 in our previous study (Yamamoto et al., 2004, 2005) (Fig. 5). We evaluated the model structures by using the PROCHEK program. Ramachandran plots of rat and human CYP24A1 showed 99% and 97% of residues either in the most favored or allowed regions, respectively. The putative structure of the active center of rat CYP24A1 was shown in Fig. 5. The A-ring and the triene part were located near the

| | | | |
|----------|-----|--|-----|
| hCYP24A1 | 1 | MSSPISKSRSLAFLQQLRSPRPQPPRLVTSTAYTSPQPREVPVCPLTAGGETQNAALPG | 60 |
| rCYP24A1 | 1 | MSCPIDKRRTLIAFLRRDLGQPPRSVTSKASASRAPEVPLCLPLMTDGETRNVTSPLG | 60 |
| CYP2C5 | 1 | MDPVVVLVLGLCCLLLS-----IWKQNSGRG-----KLPPG | 32 |
| | | *. : * : * ** | |
| | | <u>αA</u> <u>β1-1</u> <u>β1-2</u> <u>αB</u> | |
| hCYP24A1 | 61 | PTSWPLLGSLQLWKGLKQHDITLVEYHKYKQIFRMKLGFSFVHLGSPCLLEALYR | 120 |
| rCYP24A1 | 61 | PTNWPLLGSLLEIFWKGLKQHDITLAEYHKYKQIFRMKLGFSFVHLGSPCLLEALYR | 120 |
| CYP2C5 | 33 | PTPFPIIGNILQIDAKD----ISKSLTKFSECYGPFVTVYLGMPKPTVVLHGVEAVKEALV | 88 |
| | | ** : * : * : * : * : * | |
| | | <u>αB'</u> <u>SRS1</u> <u>αC</u> <u>αD</u> | |
| hCYP24A1 | 121 | TESAHPQRLKIPWKAYRDYRKEGYGLLILEGEDWQVRSAFQKKLMKPGEVMKLDNKIN | 180 |
| rCYP24A1 | 121 | TESAHPQRLKIPWKAYRDYRNEAYGLMILEGQEWQVRSAFQKKLMKPEVMKLDNKIN | 180 |
| CYP2C5 | 89 | DLGEFAGTGSVPFILEKVS---KGLGIAFSNAKTWKEMRRFSLMTLRNFGMKRSIEDRI | 145 |
| | | . * : * : * : * : * | |
| | | <u>αD</u> <u>αE</u> <u>αF</u> <u>SRS2</u> | |
| hCYP24A1 | 181 | EVLAADFMRIDELCDERGHVEDLYSELNKSFSFESICLVLYEKRFGLLQKNAGDEAVNFIM | 240 |
| rCYP24A1 | 181 | EVLADFLERMDELCDERGRIPDLYSELNKSFSFESICLVLYEKRFGLLQKETEAEALTFIT | 240 |
| CYP2C5 | 146 | QEEARCLVEELRKTN--ASPCDPTFILGCAPCNVICSVIFHNRFYKDEEFKLMEISLNE | 203 |
| | | : * : * * : * : * : * | |
| | | <u>αF</u> <u>αF'</u> <u>SRS3</u> <u>αG</u> | |
| hCYP24A1 | 241 | AIKTMSTFGRMVMT-PVELHKSLNTKVWQDHTLAWDTIFKSVKACIDNRLEKYSQQPSA | 299 |
| rCYP24A1 | 241 | AIKTMSTFGKMMVT-PVELHKSLNTKVWQDHTLAWDTIFKSVKACIDNRLEKYSQQPSA | 299 |
| CYP2C5 | 204 | NVRILSSPWLQVYNFPAALDYFPGIHKTLTKNADYIKNFIMEKVKHEKLLDVNNPRDF | 263 |
| | | : : * : * : : : : * : * : * | |
| | | <u>αH</u> <u>SRS4</u> <u>αI</u> <u>αJ</u> | |
| hCYP24A1 | 300 | DFLCDIYHQ---NRLSKKELYAAVTELQLAAVETTANSLMWILYNLSRNPQVQKLLKE | 355 |
| rCYP24A1 | 300 | DFLCDIYQQ---DHLSSKELYAAVTELQLAAVETTANSLMWILYNLSRNPQAQRLLQE | 355 |
| CYP2C5 | 264 | IDCFLIKMEQENNLEFTLESVLVAVSDLFAGAGTETTSTTLRYSLLLLKHPEVAARVQEE | 323 |
| | | * : * : * : * : * : * : * : * | |
| | | <u>αJ</u> <u>αJ'</u> <u>αK</u> <u>SRS5</u> <u>β1-4</u> <u>β2-1</u> <u>β2-2</u> <u>β1-3</u> | |
| hCYP24A1 | 356 | IQSVLPENQVPRAEDLRNMPYLKACLESMLRTPSVPF-TTRTLDKATVLGEYALPKGTV | 414 |
| rCYP24A1 | 356 | VQSVLPDNQTPRAEDLRNMPYLKACLESMLRTPSVPF-TTRTLDKPTVLGEYALPKGTV | 414 |
| CYP2C5 | 324 | IERVIGRHRSPCMQDRSRMPYTDVIEHIEQRFIDLLPTNLPHAVTRDVRFRNYFIPKGT | 383 |
| | | : : * : * : * : * : * : * : * : * : * | |
| | | <u>β1-3</u> <u>αK'</u> <u>Cys pocket</u> <u>αL</u> | |
| hCYP24A1 | 415 | ILNLNTQVLGSSDNFEDSSQFRPERWLQEKKEKIN-PFAHLPGVGKRMCI GRRLAELQLH | 473 |
| rCYP24A1 | 415 | ILNLNTQVLGSSDNFEDSHKFRPERWLQEKKEKIN-PFAHLPGVGKRMCI GRRLAELQLH | 473 |
| CYP2C5 | 384 | IITSLTSLVHDEKAFNPVKVDFPGHFLDESGNFKKSDFMPFSAGKRMVGEGLARMELF | 443 |
| | | : * : * : * : * : * : * : * | |
| | | <u>αL</u> <u>β3-3</u> <u>SRS6</u> <u>β3-2</u> | |
| hCYP24A1 | 474 | LALCWIVRKYDIQATDN---EPVEMHLGSLVPSRELPIAFQCR | 514 |
| rCYP24A1 | 474 | LALCWIIQKYDIVATDN---EPVEMHLGSLVPSRELPIAFRPR | 514 |
| CYP2C5 | 444 | LFLTSILQNFKLQSLVEPKDLDTAVVNGFVSVPPSYQLCFIPI | 487 |
| | | * * * : * : * : * : * : * : * | |

Fig. 1. Alignment of the sequences of human CYP24A1 (hCYP24A1), rat CYP24A1 (rCYP24A1), and CYP2C5. The locations and names of the helices (designated with bars) and β sheets (designated with broken bars) are shown based on the three-dimensional model. Substrate recognition sites proposed by Gotoh (1992) are in light shading, and the locations of the mutated amino acid residues are in dark shading.

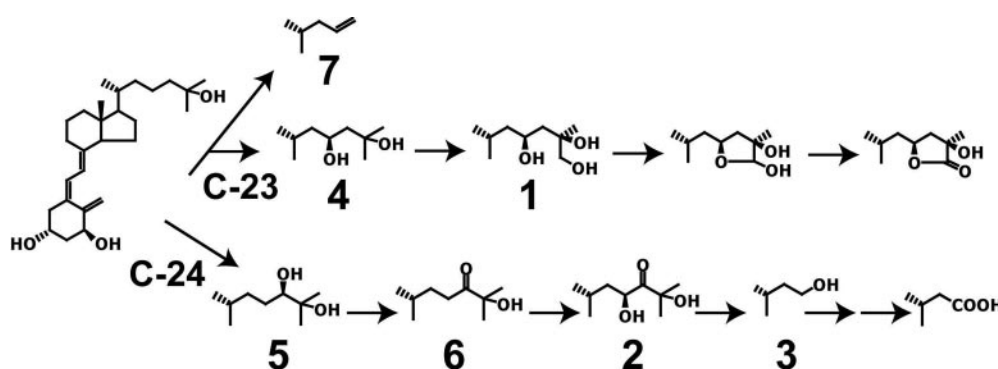


Fig. 2. Metabolic pathways of $1\alpha,25(\text{OH})_2\text{D}_3$ catalyzed by CYP24A1. Numbers indicate the metabolites shown in Figs. 3 and 4.

amino acid residues Thr416 and Ile500, respectively. The distance between oxygen atom at the side chain of Thr416 and oxygen atom at C-3 position of $1\alpha,25(\text{OH})_2\text{D}_3$ was estimated to be 6.9 Å, suggesting that no hydrogen bond was formed between either oxygen atom. The distances between Cδ of Ile500 and C-7, C-8, and C-19 of $1\alpha,25(\text{OH})_2\text{D}_3$ were estimated to 3.6, 3.5, and 3.4 Å, respectively.

Metabolism of $1\alpha,25(\text{OH})_2\text{D}_3$ by Thr416 Mutants. Figure 3 shows HPLC profiles of $1\alpha,25(\text{OH})_2\text{D}_3$ and their metabolites by Thr416 mutants. The metabolites of C-23 oxidation pathway, M1 and M7, were detected in the metabolism by the mutant T416M corresponding to human CYP24A1. In addition, the mutants T416V, T416M, T416I, and T416F had reaction specificity similar to human CYP24A1. In contrast, the metabolic pattern by the mutants T416A and T416S remains rat CYP24A1 type. Table 3 shows kinetic parameters of Thr416 mutants. The mutants T416A and T416S

showed nearly the same K_m and k_{cat} values as the wild type. On the other hand, T416M and T416V, whose enzymatic properties were similar to that of human CYP24A1 (Table 3), showed somewhat larger K_m values than human CYP24A1.

Metabolism of $1\alpha,25(\text{OH})_2\text{D}_3$ by Ile500 Mutants. Figure 3 shows HPLC profiles of $1\alpha,25(\text{OH})_2\text{D}_3$ and their metabolites by Ile500 mutants. The metabolites of C-23 oxidation pathway, M1 and M7, were detected in the metabolism by the mutants I500V, I500A, and I500L, suggesting that these mutants had reaction specificity similar to human CYP24A1. In contrast, the metabolic pattern by the mutant I500F was quite different from those of both human and rat CYP24A1. Normal-phase HPLC analysis demonstrated novel products with one hydroxyl group (Fig. 6). Mass spectrum of the metabolite UK2 is similar to that of $1\alpha,24R,25(\text{OH})_3\text{D}_3$

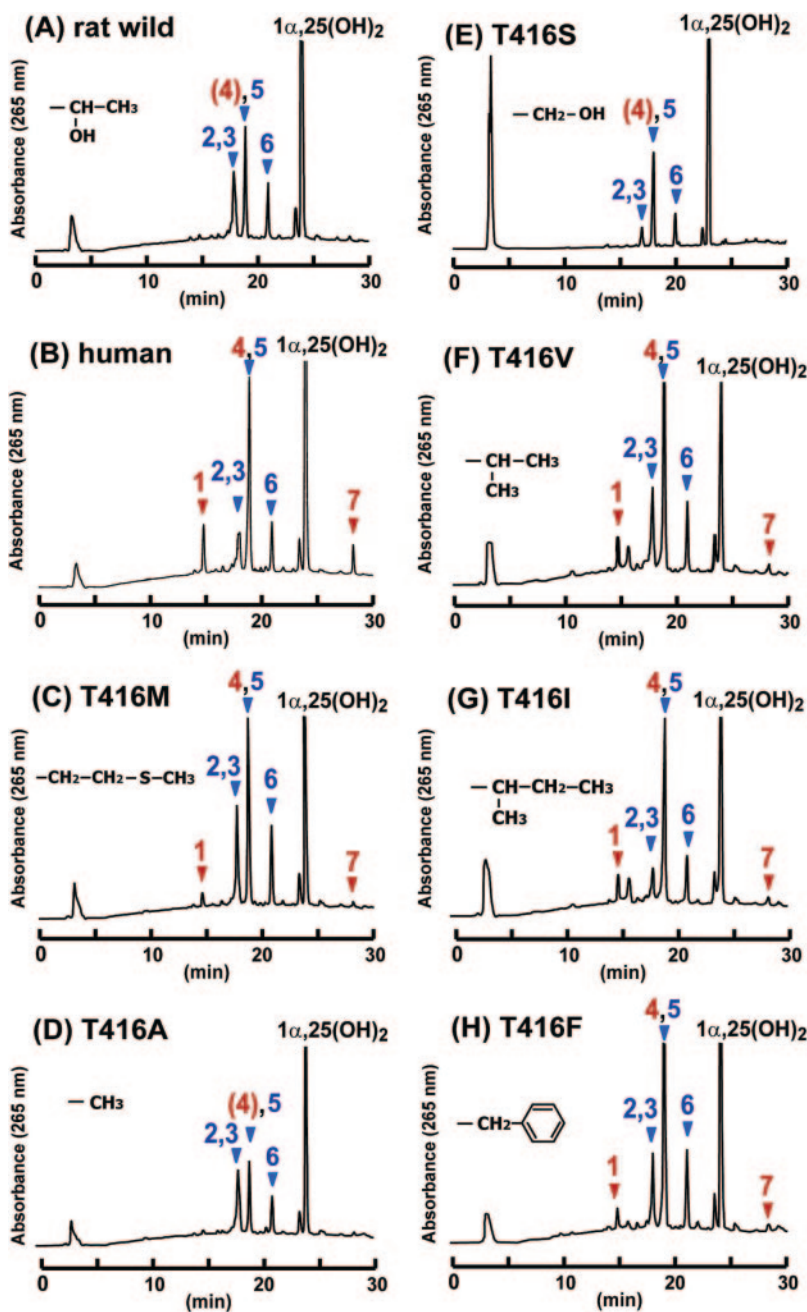


Fig. 3. HPLC profiles of $1\alpha,25(\text{OH})_2\text{D}_3$ and its metabolites by rat CYP24A1 (A), human CYP24A1 (B), and Thr416 mutants of rat CYP24A1 (C–H). After incubation with $2.0 \mu\text{M}$ $1\alpha,25(\text{OH})_2\text{D}_3$ in the presence of $2.0 \mu\text{M}$ adrenodoxin and $0.2 \mu\text{M}$ ADR for 30 min, the reaction mixture was extracted and analyzed by the reversed-phase HPLC as described under *Materials and Methods*. Numbers indicate the metabolites in C-23 (red) and C-24 (blue) oxidation pathways, as shown in Fig. 2.

with a small difference. Relative intensities (%) of major ion fragments of UK2 were as follows: m/z 361 (M+H-4H₂O), 13%; m/z 379 (M+H-3H₂O), 95%; m/z 397 (M+H-2H₂O), 100%; m/z 415 (M+H-H₂O), 87%; m/z 433 (M+H), 4.4%. On the other hand, relative intensities (%) of major ion fragments of $1\alpha,24R,25(\text{OH})_3\text{D}_3$ were as follows: m/z 361 (M+H-

4H₂O), 14%; m/z 379 (M+H-3H₂O), 92%; m/z 397 (M+H-2H₂O), 100%; m/z 415 (M+H-H₂O), 117%; m/z 433 (M+H), 6.9%. Judging from its retention time in the reversed-phase HPLC, this metabolite is neither a 26-hydroxylated product nor a 27-hydroxylated product. Although M5, the first metabolite in C-24 oxidation pathway, was observed, other me-

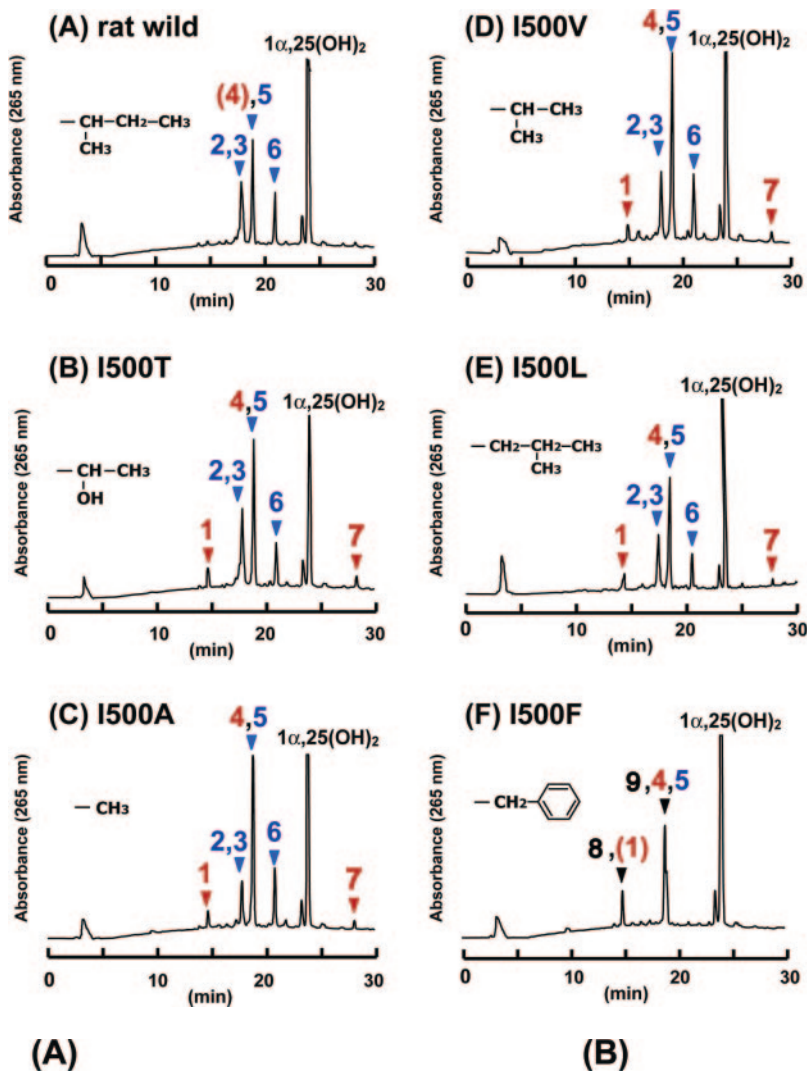


Fig. 4. HPLC profiles of $1\alpha,25(\text{OH})_2\text{D}_3$ and its metabolites by rat CYP24A1 and Ile500 mutants. After incubation with $2.0 \mu\text{M}$ $1\alpha,25(\text{OH})_2\text{D}_3$ in the presence of $2.0 \mu\text{M}$ adrenodoxin and $0.2 \mu\text{M}$ ADR for 30 min, the reaction mixture was extracted and analyzed by the reversed-phase HPLC as described under *Materials and Methods*. Numbers indicate the metabolites in C-23 (red) and C-24 (blue) oxidation pathways, as shown in Fig. 2.

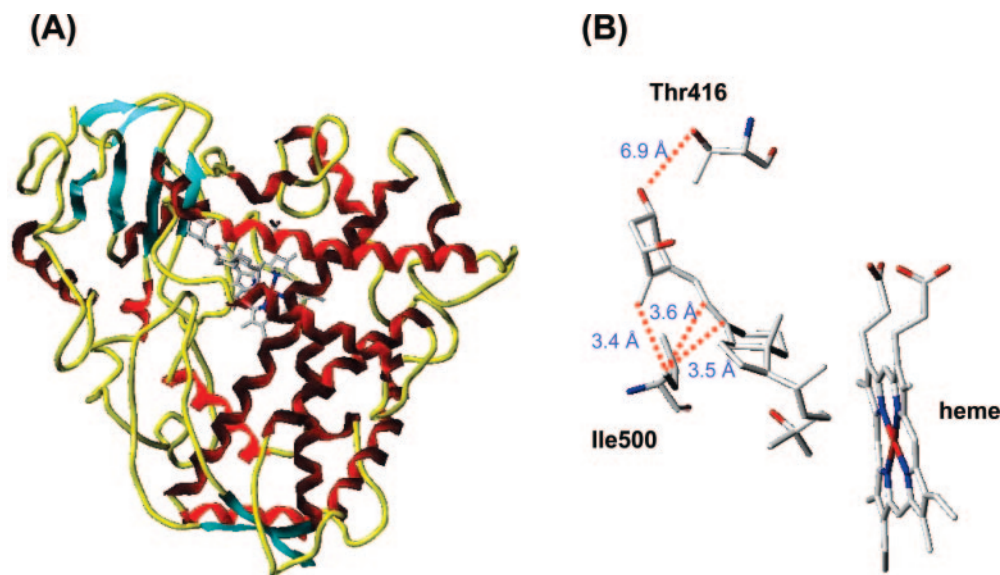


Fig. 5. Complex model of rat CYP24A1 and $1\alpha,25(\text{OH})_2\text{D}_3$ represented by ribbon-loop drawing (A), and putative location of $1\alpha,25(\text{OH})_2\text{D}_3$ and the amino acid residues, Thr416 and Ile500, in the substrate-binding pocket based on three-dimensional model of rat CYP24A1 (B). Thr416 and Ile500 were located near the A-ring and triene part, respectively. The distances between the amino acid residues and the substrate $1\alpha,25(\text{OH})_2\text{D}_3$ are indicated.

tabolites of the C-24 oxidation pathway, such as M2, M3, and M6, were not detected. On the C-23 oxidation pathway, M4 and the putative M1 were observed. However, M7 was not detected. These results strongly suggest that the amino acid residue at position 500 plays a crucial role in substrate-binding.

Discussion

CYP24A1 plays a central role in the metabolism of vitamin D and its analogs in such target tissues as kidneys, intestines, and bones. We have revealed the species-based difference on the CYP24A1-dependent metabolism of $1\alpha,25(\text{OH})_2\text{D}_3$ (Sakaki et al., 1999, 2000) and its analogs (Kusudo et al., 2003, 2004; Sakaki et al., 2003; Abe et al., 2005). Thus, information on substrate recognition and the reaction mechanism of CYP24A1 seems quite important for the development of vitamin D analogs for clinical use. Annalora et al. (2004) reported the role of Phe249 of rat CYP24A1 in substrate binding. However, this amino acid residue is conserved in rat and human CYP24A1. In this study, we attempted to identify the amino acid residues of responsible for the species-based difference between rat and human CYP24A1.

We have found that CYP3A4 shows 23 and 24-hydroxylation activity toward $1\alpha,25(\text{OH})_2\text{D}_3$ (Xu et al., 2006). However, we did not choose CYP3A4 as a template for the construction of a CYP24A1 model for the reasons described below. Although CYP3A4 shows hydroxylation activity toward a large number of compounds with different structures, CYP24A1 shows no activity toward almost all substrates of CYP3A4. CYP3A4 shows non-Michaelis-Menten kinetics and both homotropic and heterotropic cooperativity toward many substrates, suggesting that it has a noncatalytic effector site within the active site cavity. On the other hand, no reports showing atypical kinetic behaviors of CYP24A1 have been published. These results suggest that the substrate recognition of CYP3A4 is quite different from CYP24A1. Substrate specificities of CYP2A6 (Yano et al., 2005), CYP2B4 (Scott et al., 2003), and CYP2D6 (Rowland et al., 2006) are quite different from CYP24A1. Thus, we did not choose these P450s as a template. Because rat CYP2C11 shows 25-hydroxylation activity toward vitamin D_3 (Hayashi et al., 1986), it is reasonable to consider that P450s in the CYP2C family, CYP2C5 (Williams et al., 2000), 2C8 (Schoch et al., 2004), and 2C9 (Williams et al., 2003), could be template candidates for the construction of a CYP24A1 model. Our recent report indicates that a CYP27B1 model constructed using CYP2C5

as a template can fully explain our experimental data (Yamamoto et al., 2005). In addition, a CYP27A1 model constructed in a similar way can explain our experimental data (N. Sawada, K. Yamamoto, T. Sakaki, unpublished results). Note that CYP24A1 has a closer evolutionary relationship to CYP27A1 and CYP27B1 than any other P450 (Nelson et al., 2004). We have found that CYP27B1 shows 25-hydroxylation activity toward vitamin D_3 in addition to 1α -hydroxylation activity (Uchida et al., 2004). Thus, CYP27A1, CYP27B1, and CYP24A1 can add a hydroxyl group at the side chain of vitamin D_3 . Based on these facts, it is possible to assume that the tertiary structure of CYP24A1 resembles those of CYP27A1 and CYP27B1. Thus, in this study, we chose CYP2C5 as a template for the construction of a CYP24A1 model.

Our previous study on the metabolism of the A-ring diastereomers of $1\alpha,25(\text{OH})_2\text{D}_3$ suggested that amino acid residues

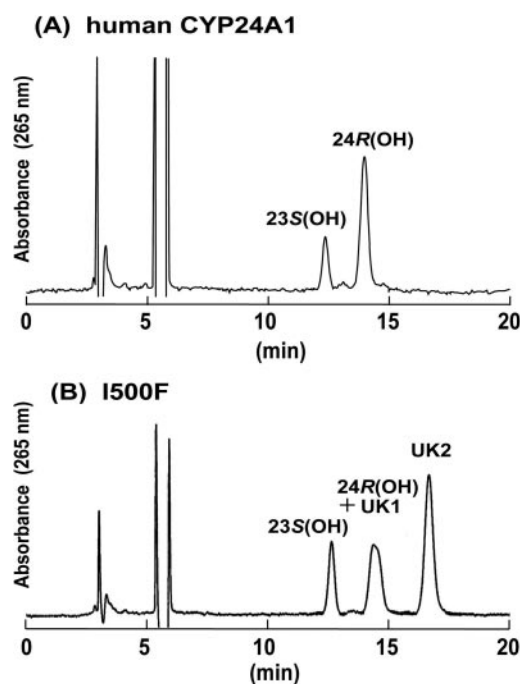


Fig. 6. Normal phase HPLC profiles of the metabolites of $1\alpha,25(\text{OH})_2\text{D}_3$ by human CYP24A1 (A) and rat CYP24A1 mutant I500F (B). The metabolites eluted at approximately 18 min with reverse phase HPLC (Fig. 3F) were collected, and analyzed using normal-phase HPLC as described under *Materials and Methods*. 23(S)(OH), 24(R)(OH), UK1, and UK2 indicate $1\alpha,23(\text{S}),25(\text{OH})_3\text{D}_3$, $1\alpha,24(\text{R}),25(\text{OH})_3\text{D}_3$, unknown metabolites 1 and 2, respectively.

TABLE 3

Kinetic parameters of wild-type and mutants CYP24A1 for $1\alpha,25(\text{OH})_2\text{D}_3$

The reaction was performed in the presence of $0.1 \mu\text{M}$ adrenodoxin, $0.01 \mu\text{M}$ ADR as described under *Materials and Methods*. Under these conditions, the sum of 23(S)-hydroxylated (M4) and 24(R)-hydroxylated (M5) products is more than 90% of total metabolites.

| CYP24A1 | Type | K_m μM | k_{cat} min^{-1} | k_{cat}/K_m |
|----------|------|------------------------|---------------------------------------|----------------------|
| Rat WT | R | 0.19 ± 0.08 | 0.26 ± 0.10 | 1.4 ± 0.1 |
| Human WT | H | 0.35 ± 0.02 | 0.43 ± 0.04 | 1.2 ± 0.1 |
| T416A | R | 0.24 ± 0.10 | 0.25 ± 0.07 | 1.2 ± 0.3 |
| T416S | R | 0.22 ± 0.01 | 0.30 ± 0.02 | 1.4 ± 0.1 |
| T416V | H | 1.04 ± 0.32 | 0.72 ± 0.31 | 0.71 ± 0.31 |
| T416M | H | 0.66 ± 0.06 | 0.21 ± 0.09 | 0.32 ± 0.15 |
| I500T | H | 0.14 ± 0.04 | 0.12 ± 0.03 | 0.92 ± 0.07 |
| I500L | H | 0.30 ± 0.12 | 0.05 ± 0.01 | 0.17 ± 0.03 |
| I500F | N | 1.14 ± 0.40 | 0.11 ± 0.04 | 0.10 ± 0.04 |

R, H, and N indicate rat-, human-, and novel-type metabolism, respectively.

interacting with the A-ring of the substrate contributed to species-based difference between rat and human CYP24A1 (Kusudo et al., 2004). In addition, our recent studies revealed that Thr409 of CYP27B1 is responsible for substrate binding, probably because of hydrogen bond formation between the OH group of Thr409 and 25(OH)₂ group of 1 α ,25(OH)₂D₃ (Yamamoto et al., 2005). Amino acid sequence alignments indicated that Thr416 of rat CYP24A1 and Met416 of human CYP24A1 correspond to Thr409 of human CYP27B1. Although the substrate is inserted in an opposite direction between CYP27B1 and CYP24A1, we examined whether Thr416 is involved in substrate binding. The docking model of CYP24A1 and 1 α ,25(OH)₂D₃ indicated that the A-ring of 1 α ,25(OH)₂D₃ could be located near the amino acid residue at position 416. Thus, we expressed T416M in *E. coli* cells and examined its enzymatic properties. As expected, the metabolic pattern of 1 α ,25(OH)₂D₃ by mutant T416M resembled human CYP24A1. The ratio of C-23 to C-24 oxidation pathway on T416M was estimated to be 0.08, which was much higher than the wild type of rat CYP24A1 (0.01). Note that animal species with a high ratio of C-23 to C-24 oxidation pathway, such as chicks and humans, have Met at position 416, whereas those with low C-23 ratio, such as rats and mice, have Thr at position 416 (Portale and Miller, 2000).

Although Thr416 is near the A-ring, judging from the distance (6.9 Å) between the oxygen atoms, no hydrogen bond can be formed between the oxygen atom on the side chain of Thr416 and the oxygen atom at the C-3 position of 1 α ,25(OH)₂D₃ (Fig. 5). Both T416S and T416A showed only C-24 pathway (rat type) with nearly the same affinity for 1 α ,25(OH)₂D₃ as the wild type. On the other hand, Thr416 mutants replaced by such large and hydrophobic amino acids as Met, Val, Ile, and Phe showed both C-23 and C-24 oxidation pathways (human type). The fact that T416V showed human-type metabolism demonstrates that a difference between the hydroxyl group (Thr) and the methyl group (Val) determines the metabolic pattern of 1 α ,25(OH)₂D₃. At the present stage, we cannot clearly explain these results from the complex model of CYP24A1 and 1 α ,25(OH)₂D₃. However, it might be possible to assume that a few water molecules form a hydrogen-bond network between the OH group of the amino acid at position 416 and 3 β -OH group of 1 α ,25(OH)₂D₃. The hydroxyl group of Thr or Ser is involved in the hydrogen bond network. Based on the speculation that Ala cannot remove a putative water molecule bound to the 3 β -OH group of 1 α ,25(OH)₂D₃, whereas Met, Val, Ile, and Phe remove the water molecule to disrupt the hydrogen bond network, the mutation to the larger hydrophobic residues and removal of water seem to be associated with the shift in metabolism down the C-23 pathway.

Of the seven mutants in the SRS regions (Fig. 1), only I500T showed human-type metabolic pattern. Based on the three-dimensional model of rat CYP24A1, Ile500 was located near the triene part of 1 α ,25(OH)₂D₃. The distances between C δ of Ile 500 and C-7, C-8, and C-19 of 1 α ,25(OH)₂D₃ were estimated to 3.6, 3.5, and 3.4 Å, respectively (Fig. 5). In addition to I500T, mutants I500A, I500V, and I500L also showed a metabolic pattern similar to that of human CYP24A1. These results reveal that rat CYP24A1-type metabolism is specifically observed when the amino acid at 500 is Ile. Note that I500L and I500V have a human-type metabolic pattern, suggesting that positional change or deletion of

one methyl group can change the ratio between C-23 and C-24 oxidation pathways. The ratio between C-23 and C-24 oxidation pathways of I500T was estimated to be 0.16, which was much higher than that of wild-type rat CYP24A1 (0.01) and significantly higher than T416M (0.08).

One of the most interesting findings in this study is the reaction specificity of the mutant I500F. In addition to 24(R)-hydroxylated (M5) and 23(S)-hydroxylated (M4) products, unknown product UK2 was observed as a major metabolite. Judging from its retention time in reversed-phase HPLC, UK2 is neither a 26-hydroxylated product nor a 27-hydroxylated product. Two major metabolites of 1 α ,25(OH)₂D₃ by CYP3A4, which are considered to be 23(R)- and 24(S)-hydroxylated products, showed different retention times from UK2 (Xu et al., 2006). Based on these results, UK2 might have a hydroxyl group at a novel position such as C-22. Metabolic analysis and kinetic studies suggest that the substrate-binding pocket of I500F is quite different from those of both rat and human CYP24A1.

To the best of our knowledge, this is the first report to show the amino acid residues of CYP24A1 responsible for its reaction specificity. Naturally occurring one-point mutation is adequate to change the ratio between C-23 and C-24 oxidation pathways. Such metabolites as 24(R),25(OH)₂D₃ (Corvol et al., 1978; Henry and Norman, 1978; Ornoy et al., 1978) and 1 α ,25(OH)₂D₃-26,23-lactone (Shima et al., 1990) have been reported to be biologically active. Thus, the change of the ratio between C-23 and C-24 oxidation pathways seems to have biological significance.

Our findings indicate that the substitution of one nucleotide of rat *CYP24A1* gene can produce human-type CYP24A1. Thus, it might be possible to generate a "humanized rat" on CYP24A1-dependent metabolism by homologous recombination. Humanized rats or mice would be useful to predict the metabolism of vitamin D analogs in humans.

References

- Abe D, Sakaki T, Kusudo T, Kittaka A, Saito N, Suhara Y, Fujishima T, Takayama H, Hamamoto H, Kamakura M, et al. (2005) Metabolism of 2 α -propoxy-1 α ,25-dihydroxyvitamin D₃ and 2 α -(3-hydroxypropoxy)-1 α ,25-dihydroxyvitamin D₃ by human CYP27A1 and CYP24A1. *Drug Metab Dispos* 33:778–784.
- Akiyoshi-Shibata M, Sakaki T, Ohyama Y, Noshiro M, Okuda K, and Yabusaki Y (1994) Further oxidation of hydroxycalcidol 24-hydroxylase: a study with the mature enzyme expressed in *Escherichia coli*. *Eur J Biochem* 224:335–343.
- Annalora A, Bobrovnikova-Marion E, Serda R, Lansing L, Chiu ML, Pastuszyn A, Iyer S, Marcus CB, and Omdahl JL (2004) Rat cytochrome P450C24 (CYP24A1) and the role of F249 in substrate binding and catalytic activity. *Arch Biochem Biophys* 425:133–146.
- Beckman MJ, Tadikonda P, Werner E, Prah J, Yamada S, and DeLuca HF (1996) Human 25-hydroxyvitamin D₃-24-hydroxylase, a multicatalytic enzyme. *Biochemistry* 35:8465–8472.
- Binderup L (1992) Immunological properties of vitamin D analogues and metabolites. Immunological properties of vitamin D analogues and metabolites. *Biochem Pharmacol* 43:1885–1892.
- Binderup L, Latini S, Binderup E, Bretting C, Calverley M, and Hansen K (1991) 20-epi-vitamin D₃ analogues: a novel class of potent regulators of cell growth and immune responses. *Biochem Pharmacol* 42:1569–1575.
- Bouillon R, Okamura WH, and Norman AW (1995) Structure-function relationships in the vitamin D endocrine system. *Endocr Rev* 16:200–257.
- Boyle IT, Gray RW, and DeLuca HF (1971) Regulation by calcium of in vivo synthesis of 1,25-dihydroxycholecalciferol and 21,25-dihydroxycholecalciferol. *Proc Natl Acad Sci USA* 68:2131–2134.
- Corvol MT, Dumontier MF, Garabedian M, and Rappaport R (1978) vitamin D and cartilage. II. Biological activity of 25-hydroxycholecalciferol and 24,25- and 1,25-dihydroxycholecalciferols cultured growth plate chondrocytes. *Endocrinology* 102:1269–1274.
- Dilworth FJ, Williams GR, Kissmeyer AM, Nielsen JL, Binderup E, Calverley MJ, Makin HL, and Jones G (1997) The vitamin D analog KH1060, is rapidly degraded both in vivo and in vitro via several pathways: principal metabolites generated retain significant biological activity. *Endocrinology* 138:5485–5496.
- Gotoh O (1992) Substrate recognition sites in cytochrome P450 family 2 (CYP2) proteins inferred from comparative analyses of amino acid and coding nucleotide sequences. *J Biol Chem* 267:83–90.

- Hayashi S, Noshiro M, and Okuda K (1986) Isolation of a cytochrome P-450 that catalyzes the 25-hydroxylation of vitamin D₃ from rat liver microsomes. *J Biochem* **99**:1753–1763.
- Henry HL and Norman AW (1978) Vitamin D: two dihydroxylated metabolites are required for normal chicken egg hatchability. *Science (Wash DC)* **201**:835–837.
- Hiwatashi A, Nishii Y, and Ichikawa Y (1982) Purification of cytochrome P-450D 1 α (25-hydroxyvitamin D₃-1 α -hydroxylase) of bovine kidney mitochondria. *Biochem Biophys Res Commun* **105**:320–327.
- Holick MF, Schnoes HK, and DeLuca HF (1971) Identification of 1,25-dihydroxycholecalciferol, a form of vitamin D₃ metabolically active in the intestine. *Proc Natl Acad Sci USA* **68**:803–804.
- Kahraman M, Sinishtanj S, Dolan PM, Kessler TW, Peleg S, Saha U, Chung SS, Bernstein G, Korczak B, and Posner GH (2004) Potent, selective and low-calcemic inhibitors of CYP24 hydroxylase: 24-sulfoximine analogues of the hormone 1 α ,25-dihydroxyvitamin D(3). *J Med Chem* **47**:6854–6863.
- Kondo S, Sakaki T, Ohkawa H, and Inouye K (1999) Electrostatic interaction between cytochrome P450 and NADPH-P450 reductase: comparison of mixed and fused systems consisting of rat cytochrome P450 1A1 and yeast NADPH-P450 reductase. *Biochem Biophys Res Commun* **257**:273–278.
- Kusudo T, Sakaki T, Abe D, Fujishima T, Kittaka A, Takayama H, Hatakeyama S, Ohta M, and Inouye K (2004) Metabolism of A-ring diastereomers of 1 α ,25-dihydroxyvitamin D₃ by CYP24A1. *Biochem Biophys Res Commun* **321**:774–782.
- Kusudo T, Sakaki T, Abe D, Fujishima T, Kittaka A, Takayama H, Ohta M, and Inouye K (2003) Metabolism of 20-epimer of 1 α ,25-dihydroxyvitamin D₃ by CYP24, species-based difference between humans and rats. *Biochem Biophys Res Commun* **309**:885–892.
- Lawson DE, Fraser DR, Kodicek E, Morris HR, and Williams DH (1971) Identification of 1,25-dihydroxycholecalciferol, a new kidney hormone controlling calcium metabolism. *Nature (Lond)* **230**:228–230.
- Lowry OH, Rosebrough NJ, Farr AL, and Randall RJ (1951) Protein measurement with the Folin phenol reagent. *J Biol Chem* **193**:265–275.
- Nelson DR, Zeldin DC, Hoffman SM, Maltais LJ, Wain WH, and Nebert DW (2004) Comparison of cytochrome P450 (CYP) genes from the mouse and human genomes, including nomenclature recommendations for genes, pseudogenes and alternative-splice variants. *Pharmacogenetics* **14**:1–18.
- Norman AW, Myrtle JF, Midgett RJ, Nowicki HG, Williams V, and Popjak G (1971) 1,25-Dihydroxycholecalciferol: identification of the proposed active form of vitamin D₃ in the intestine. *Science (Wash DC)* **173**:51–54.
- Omdahl JL, Bobrovnikova EV, Annalora A, Chen P, and Serda R (2003) Expression, structure-function and molecular modeling of vitamin D P450s. *J Cell Biochem* **88**:356–362.
- Omura T and Sato R (1964) The carbon monoxide-binding pigment of liver microsomes. II. Solubilization, purification, and properties. *J Biol Chem* **239**:2379–2385.
- Ornoff A, Goodwin D, Noff D, and Edelstein S (1978) 24,25-Dihydroxyvitamin D is a metabolite of vitamin D essential for bone formation. *Nature (Lond)* **276**:517–519.
- Portale AA and Miller WL (2000) Human 25-hydroxyvitamin D-1 α -hydroxylase: cloning, mutations and gene expression. *Pediatr Nephrol* **14**:620–625.
- Rowland P, Blaney FE, Smyth MG, Jones JJ, Leydon VR, Oxbrow AK, Lewis CJ, Tennant MG, Modi S, Eggleston DS, et al. (2006) Crystal structure of human cytochrome P450 2D6. *J Biol Chem* **281**:7614–7622.
- Sakaki T, Sawada N, Abe D, Komai K, Shiozawa S, Nonaka Y, Nakagawa K, Okano T, Ohta M, and Inouye K (2003) 26,26,26,27,27,27-F₆-1 α , 25-dihydroxyvitamin D₃ by CYP24: species-based difference between humans and rats. *Biochem Pharmacol* **65**:1957–1965.
- Sakaki T, Sawada N, Komai K, Shiozawa S, Yamada S, Yamamoto K, Ohyama Y, and Inouye K (2000) Dual metabolic pathway of 25-hydroxyvitamin D₃ catalyzed by human CYP24. *Eur J Biochem* **267**:6158–6165.
- Sakaki T, Sawada N, Nonaka Y, Ohyama Y, and Inouye K (1999) Metabolic studies using recombinant *Escherichia coli* cells producing rat mitochondrial CYP24. *Eur J Biochem* **262**:43–48.
- Sawada N, Kusudo T, Sakaki T, Hatakeyama S, Hanada M, Abe D, Kamao M, Okano T, Ohta M, and Inouye K (2004) Novel metabolism of 1 α ,25-dihydroxyvitamin D₃ with C24–C25 bond cleavage catalyzed by human CYP24A1. *Biochemistry* **43**:4530–4537.
- Scott EE, He YA, Wester MR, White MA, Chin CC, Halpert JR, Johnson EF, and Stout CD (2003) An open conformation of mammalian cytochrome P450 2B4 at 1.6-Å resolution. *Proc Natl Acad Sci USA* **100**:13196–13201.
- Schoch GA, Yano JK, Wester MR, Griffin KJ, Stout CD, and Johnson EF (2004) Structure of human microsomal cytochrome P450 2C8: evidence for a peripheral fatty acid binding site. *J Biol Chem* **279**:9497–9503.
- Schuster I, Egger H, Nussbaumer P, and Kroemer RT (2003) Inhibitors of vitamin D hydroxylases: structure-activity relationships. *J Cell Biochem* **88**:372–380.
- Shima M, Tanaka H, Norman AW, Yamaoka K, Yoshikawa H, Takaoka K, Ishizuka S, and Seino Y (1990) 23(S),25(R)-1,25-Dihydroxyvitamin D₃-26,23-lactone stimulates murine bone formation in vivo. *Endocrinology* **126**:832–836.
- Uchida E, Kagawa N, Sakaki T, Urushino N, Sawada N, Kamakura M, Ohta M, Kato S, and Inouye K (2004) Purification and characterization of mouse CYP27B1 overproduced by an *Escherichia coli* system coexpressing molecular chaperonins GroEL/ES. *Biochem Biophys Res Commun* **323**:505–511.
- Wester MR, Johnson EF, Marques-Soures C, Danette PM, Mansuy D, and Stout C (2003) Structure of a substrate complex of mammalian cytochrome P450 2C5 at 2.3 Å resolution: evidence for multiple substrate binding modes. *Biochemistry* **42**:6370–6379.
- Williams PA, Cosme J, Sridhar V, Johnson EF, and McRee DE (2000) Mammalian microsomal cytochrome P450 monooxygenase: structural adaptations for membrane binding and functional diversity. *Mol Cell* **5**:121–131.
- Williams PA, Cosme J, Vinkovic DM, Ward A, Angove HC, Day PJ, Vornrhein C, Tickle IJ, and Jhoti H (2004) Crystal structures of human cytochrome P450 3A4 bound to metyrapone and progesterone. *Science (Wash DC)* **305**:683–686.
- Williams PA, Cosme J, Ward A, Angove H, Matak C, Vinkovic D, and Jhoti H (2003) Crystal structure of human cytochrome P450 2C9 with bound warfarin. *Nature (Lond)* **424**:464–468.
- Xu Y, Hashizume T, Shuhart MC, Davis CL, Nelson WL, Sakaki T, Kalhorn TF, Watkins PB, Schuetz EG, and Thummel KE (2006) Intestinal and hepatic CYP3A4 catalyze hydroxylation of 1 α ,25-dihydroxyvitamin D₃: implications for drug-induced osteomalacia. *Mol Pharmacol* **69**:56–65.
- Yamamoto K, Masuno H, Sawada N, Sakaki T, Inouye K, Ishiguro M, and Yamada S (2004) Homology modeling of human 25-hydroxyvitamin D₃ 1 α -hydroxylase (CYP27B1) based on the crystal structure of rabbit CYP2C5. *J Steroid Biochem Mol Biol* **89**:167–171.
- Yamamoto K, Uchida E, Urushino N, Sakaki T, Kagawa N, Sawada N, Kamakura M, Kato S, Inouye K, and Yamada S (2005) Identification of the amino acid residue of CYP27B1 responsible for binding of 25-hydroxyvitamin D₃ whose mutation causes vitamin D-dependent rickets type 1. *J Biol Chem* **280**:30511–30516.
- Yano JK, Hsu M, Griffin KJ, Stout CD, and Johnson EF (2005) Structure of human microsomal cytochrome P450 2A6 complexed with coumarin and methoxsalen. *Nat Struct Mol Biol* **12**:822–823.

Address correspondence to: Toshiyuki Sakaki, Biotechnology Research Center, Faculty of Engineering, Toyama Prefectural University, 5180 Kurokawa, Imizu, Toyama 939-0398, Japan. E-mail: tsakaki@pu-toyama.ac.jp